ISSN 1063-7842, Technical Physics, 2008, Vol. 53, No. 11, pp. 1407–1413. © Pleiades Publishing, Ltd., 2008.
Original Russian Text © Yu.K. Stishkov, V.A. Chirkov, 2008, published in Zhurnal Tekhnicheskoĭ Fiziki, 2008, Vol. 78, No. 11, pp. 17–23.

GASES AND LIQUIDS

Computer Simulation of EHD Flows in a Needle–Plane Electrode System

Yu. K. Stishkov and V. A. Chirkov

Electrophysics Research and Education Center, St. Petersburg State University, St. Petersburg, 198504 Russia

Received November 29, 2007

Abstract—Complex investigation of the structure of electrohydrodynamic (EHD) flows in a needle–plane electrode system is carried out on the basis of analysis of experimental data and the results of computer simulation. An algorithm of iterative simulation of the volume charge distribution in a fluid is developed. Simulation is carried out using the ANSYS system. The fields of velocities and pressures, as well as electric characteristics of EHD flows, are calculated. Analysis of the results reveals a number of features of EHD flows in the electrode system under investigation. Peculiarities of the band structure are determined, and the characteristic size of the low-pressure zone near the active electrode, as well as the sizes of the acceleration and deceleration zones of the fluid in the electrode gap, is determined.

PACS numbers: 47.65.-d

DOI: 10.1134/S1063784208110030

INTRODUCTION

The unified system of electrohydrodynamics (EHD) reflects close interrelation of the phenomena of conduction and charge formation with hydrodynamics. The relation between variables (electric field, charge, current, velocity, pressure, etc.) is essentially nonlinear; for this reason, the system of equations cannot be solved analytically. These equations can be analyzed only in certain approximations, in simplified formulations under certain assumptions. To formulate simplifying assumptions required for obtaining a theoretical description and for revealing physical foundations of a process, numerical simulation of EHD problems is carried out along with experimental investigations. To find out whether the assumptions made in the formulation of the problem are valid, it is necessary to compare the results of simulation with experimental data. Experiments aimed at studying EHD flows in different geometries, with different fluids, and under various boundary and initial conditions help to determine the applicability of the model used for describing EHD flows, to find the range in which it matches the observed phenomena, and ultimately to refine the model.

Until recently, two-dimensional (2D) EHD flows emerging in a system of electrodes consisting of a cylinder above a plane or of two cylinders have been investigated [1–3]. At the same time, EHD flows in the needle–plane electrode system are encountered most frequently in engineering. In this system, much higher velocities of the fluid flow and much larger pressure gradients are observed for the same voltage, radii of curvature of active electrodes, and for the same electrode spacing [4].

This study aims at experimental investigation of peculiarities of EHD flows in a needle–plane electrode system and at computer simulation of the process under analogous conditions. The model studied here is axisymmetric. It consists of a cylindrical cell containing an active and a passive electrode (a needle and a plane, respectively).

SIMULATION

Taking into account the axial symmetry of the system under investigation, a 2D axisymmetric finite-element model was constructed. The geometry of the model (Fig. 1) is close to the geometry of experiment (a cylinder of height $d = 20$ mm and diameter $2b = 30$ mm, containing a needle with a base diameter of 0.2 mm and a radius of the tip curvature $r = 0.1$ mm; the spacing between the electrodes is $a = 7$ mm). The fluid under investigation was transformer oil with the following properties: electrical conductivity $\sigma = 10^{-12}$ Ω^{-1} m^{-1}, relative permittivity $\varepsilon = 2.2$, mechanical density $\gamma = 850$ kg/m^3, and dynamic viscosity $\eta = 0.02$ Pa s. The output data of the simulation program are the voltage across the electrodes, the conditions at the walls of the model, the volume charge density and its initial distribution. The boundary conditions are shown in Fig. 1. The potential difference between the electrodes is 5 kV. The volume charge density is 0.15 C/m^3.

Let us compare the drift velocity of ions and the velocity of the fluid flow in the main region of the electrode gap; i.e., we estimate the value of the electrical Reynolds number defined by the formula

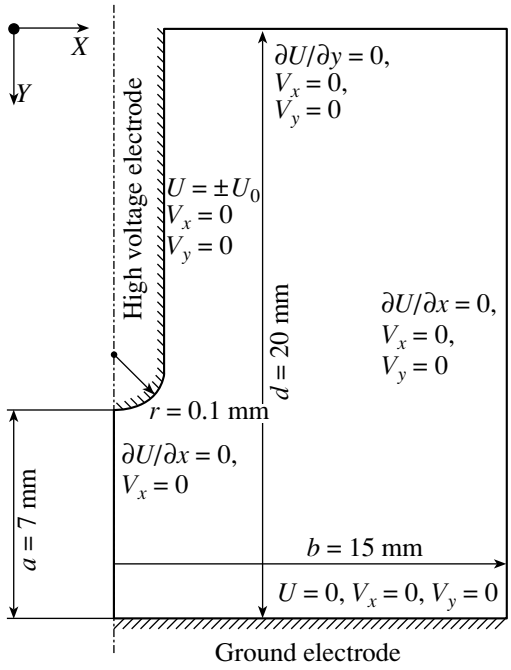

Fig. 1. Boundary conditions and geometry of the computer model (U is the potential and V_x, V_y are the x and y components of the velocity).

$$\mathrm{Re}_{\mathrm{el}} = \frac{v_{\mathrm{fluid}}}{b_i E},$$

where v_{fluid} is the characteristic velocity of the fluid, b_i is the mobility of ions, and E is the electric field strength.

In this problem (as will be shown below), the velocities are of the same order of magnitude (10^{-1} m/s), the mobility of ions in transformer oil is estimated as 10^{-8} m^2/(V s), and the typical value of electric field is 10^6 V/m. Thus, the characteristic value of the electrical Reynolds number is on the order of 10. Consequently, the velocity of the fluid considerably exceeds the average drift velocity of ions and, hence, we can assume that the ions forming the volume charge are "frozen" in the fluid and move along the flow lines. The formation of solvate envelopes [5] is one of the known mechanisms of freezing ions in the fluid.

In this model, we assume that the charge distribution in a charged filament is uniform (i.e., the value of density is constant in the region with the volume charge). This assumption is justified if ions are frozen in the fluid. In this case, the charge moves along the flow lines and, hence, its density remains unchanged (in the case of an incompressible fluid) over the entire electrode gap. It should also be noted that in this approximation, a filament of the EHD flow contains charge of the same polarity (coinciding with the polarity of the active electrode) and, hence, recombination processes in the region of the central filament are absent and cannot change the charge density in the filament.

We used an iterative algorithm for simulating a charged filament. In the first step, the test distribution of volume charge was defined in the region around the needle electrode and in the electrode gap. The region with volume charge in the electrode gap was a cylinder coaxial with the symmetry axis of the model and having a radius $R_c = sR_n$, where R_n is the radius of the needle tip and s is a parameter corresponding to the width of the charged region. The region of volume charge was corrected between interactions only in the electrode gap and remained unchanged around the needle electrode. The main criterion for estimating the solution was the conservation of convective current in profile cross sections of the model. The convective current was calculated by the formula

$$I = \int_0^{R_c} v\rho 2\pi r dr = \rho \int_0^{R_c} v 2\pi r dr,$$

where v is the projection of the fluid velocity onto the symmetry axis and ρ is the volume charge density. The integral was evaluated over the line lying in the profile cross section from the symmetry axis to the boundary of the volume charge region. Taking into account the initial assumption concerning the invariability of volume charge density ρ in the cross-section plane, the density can be taken out of the integral. In this case, the current is the product of the fluid flow rate through the cross-sectional area element of radius R_c and charge density ρ. Consequently, the conservation of current in the profile cross sections is equivalent to the conservation of the fluid flow rate. Consequently, to improve the solution in accordance with the above criterion, it is necessary that the volume charge boundary coincides with the fluid flow line obtained precisely for the given charge distribution.

Proceeding from the above line of reasoning, we performed the following procedure to find the optimal solution. After the first step in the solution of the problem, we determined the coordinates of the flow line (with a fixed initial point at the boundary of the volume charge region), which were written in the file. The point on the volume charge boundary, from which the flow line (to be more precise, distance R_c from this point to the axis) was determined is a free parameter of the problem. However, this parameter can vary only prior to the beginning of the entire solution and remains unchanged between iterations. In the second step of the solution (second iteration), the volume charge density was specified in the region between the symmetry axis of the model and the obtained flow line. Taking into account these circumstances, the value of R_c used for determining the current in the cross sections (evaluation of the corresponding integral) was controlled by the level of the specific cross section and depended on the coordinate of the flow line obtained at the previous iteration. For obtaining a new solution and a new con-

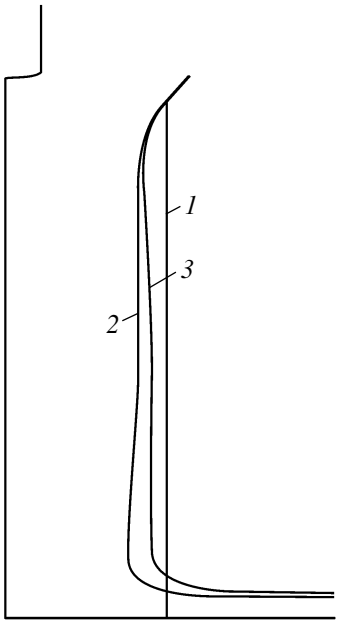

Fig. 2. Boundaries of the charged region (*1*) after the first (*2*) and fifth (*3*) iterations.

figuration of the flow line, the described procedure was repeated.

To control the above criterion for estimating the convergence of the solution in the course of calculations, profile cross sections at levels of 0.1, 0.2, …, 0.9 of the electrode gap were used. The algorithm developed here makes it possible to obtain a solution with an invariable arrangement of flow lines already after the fifth iteration. The chosen criterion of conservation of current after five iterations for the cross section at levels of 0.7 and 0.9 of the electrode gap was satisfied to an extent of 99 and 96%, respectively (at a voltage of 5 kV).

Figure 2 shows the boundaries of the charged region after the first and fifth iterations. For better visualization, the scale of the figure on the horizontal axis was magnified fivefold as compared to the vertical axis. A charged filament has a funnel-shaped narrowing immediately under the needle electrode and has the shape of an almost regular cylinder (the cross section of which varied to within 5%) in the far-field zone. The iterative process converges quite rapidly and the difference between the last two iterations is insignificant.

RESULTS OF COMPUTER SIMULATION AND DISCUSSION

Let us consider the results. Figure 3 shows the axial and profile distributions of velocities.

It can be seen from Fig. 3a that the axial distribution of the velocity has a peak at 0.2 of the electrode gap. The most intense acceleration takes place in the immediate vicinity of the active electrode (Fig. 4a). It is followed by the region of quasi-uniform flow—the absolute value of acceleration in the most part of the electrode gap is much smaller than in the electrode regions and the fluid flows uniformly at an average velocity of 35 cm/s. The second lower velocity peak, which is associated with an increase in the electric field strength near the earthed electrode under the action of the incoming volume charge (and, hence, with the increase in the volume forces acting on the fluid), is observed at the counter electrode. The appreciable decrease in the magnitude of velocity is observed immediately at the surface of the counter electrode, which can be explained by a sharp change in the direction of the flow of a charged filament. The half-width of the graph of the velocity profile is approximately seven radii of the needle (the horizontal axes of the graphs in Figs. 3b and 4b are normalized to the radius of the needle electrode). It can be seen that high velocities of the flow are characteristic only of a narrow central cylindrical filament, while the velocities in the remaining part of the cell are much lower.

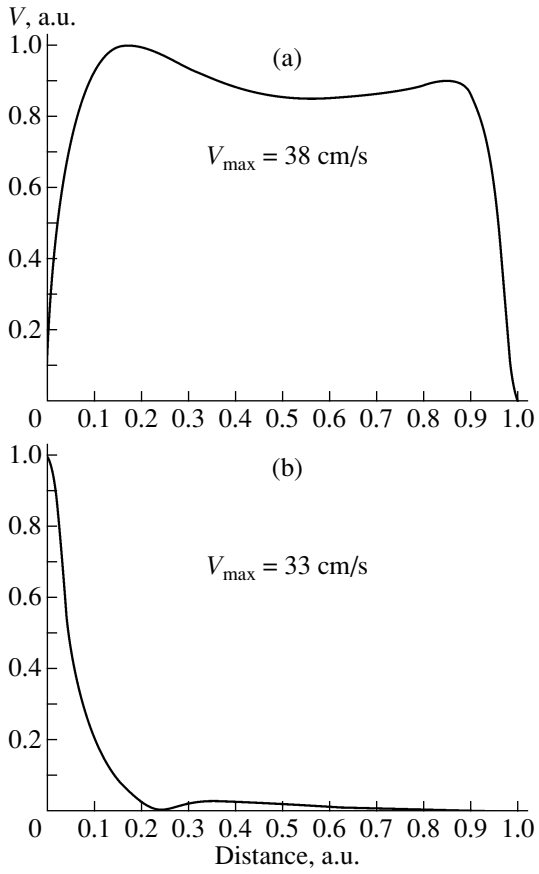

Fig. 3. (a) Axial distribution of the magnitude of velocity and (b) the profile of the *y* component of the velocity at the middle of the electrode gap.

Figure 4b shows the dependence of the derivative of the longitudinal velocity component with respect to the transverse coordinate. The kink on the transverse derivative is a characteristic feature of the transition from the

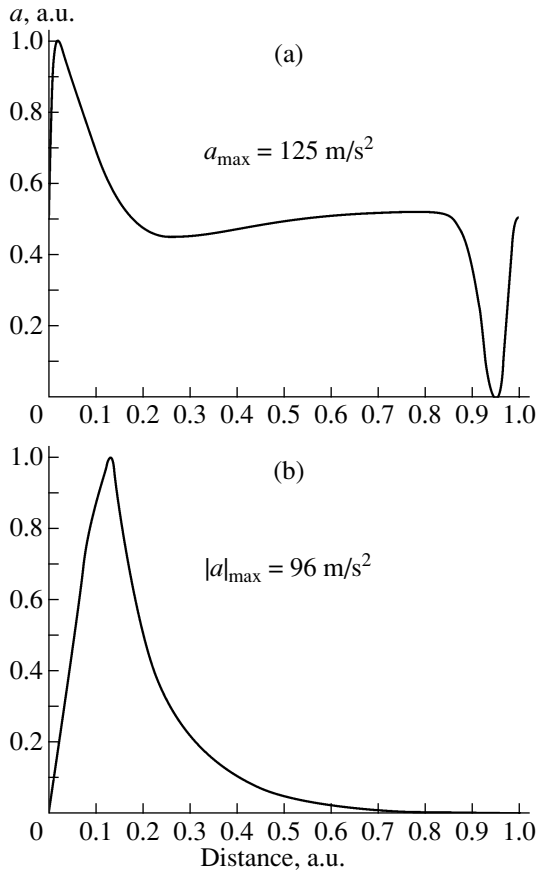

Fig. 4. (a) Derivative of the axial velocity graph and (b) the magnitude of the derivative of the profile of the y component of velocity at the middle of the electrode gap.

force flow in the filament to a viscous flow outside it. In electrohydrodynamics, the force part of the flow coincides with the region of localization of the volume charge [6]. Analysis of experimental data on the basis of this property makes it possible to determine the thickness of the charged filament, which was used for simulation. The characteristic point of the kink on the graph obtained as a result of simulation lies at a distance of four radii of the needle electrode from the axis and corresponds to the preset boundary of the charged region.

Figure 5a shows the contour diagram of pressure under the needle electrode. The low-pressure region located immediately under the needle electrode almost coincides with the boundaries of the charged ribbon surrounding the needle electrode. The pressure along the remaining part of the electrode gap is slightly lower. This can be clearly traced on the linear pressure graph (Fig. 6b). Figure 5b shows the map of velocity level lines in the EHD flow. A layer of stationary fluid lies immediately at the surface of the needle electrode. The fluid is strongly accelerated along the axis, and the flow velocity rapidly decreases with increasing distance from the axis in the transverse direction.

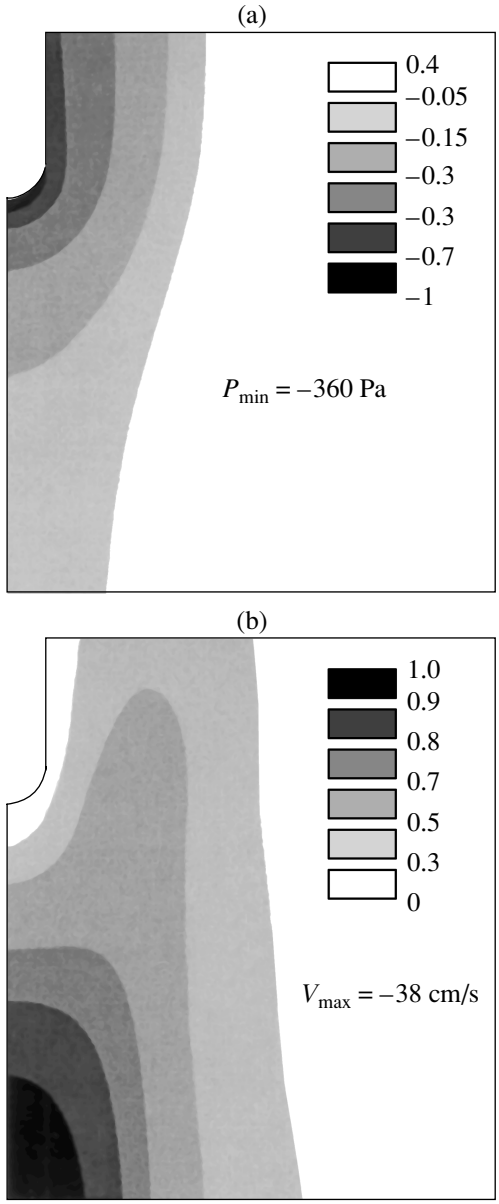

Fig. 5. Contour diagrams of (a) pressure and (b) velocity near the surface of the needle electrode.

Figure 6a shows the graphs of the densities of the Coulomb ($E_{electric}$) and hydrodynamic (E_{hydro}) forces. The densities of the forces were calculated using the formulas

$$F_{electric} = \rho E,$$

$$F_{hydro} = \gamma a,$$

where ρ is the volume charge density, γ is the mechanical density of the fluid, E is the electric field, and a is the acceleration of the fluid. In the initial and final segments, the difference in forces is due to large pressure gradients: under the action of Coulomb forces, the fluid flows from the region with a lower pressure to that with

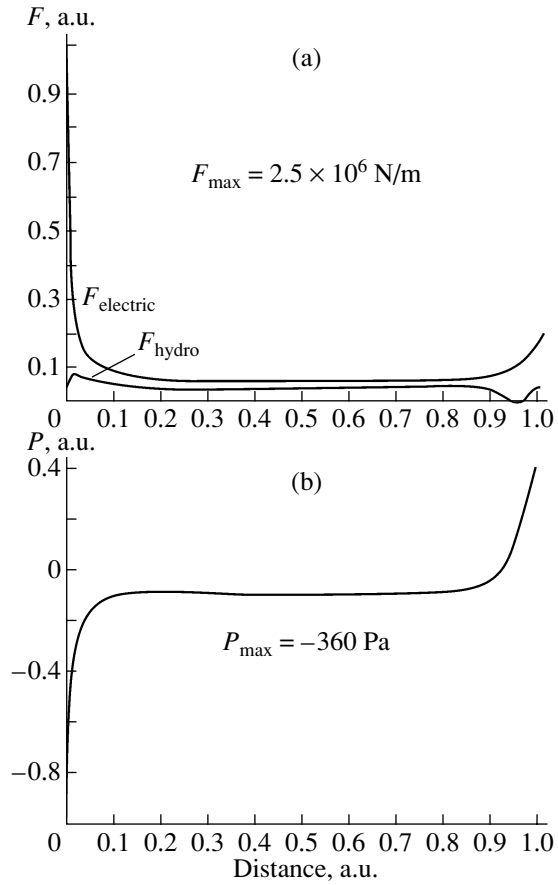

Fig. 6. Axial graphs of the densities of (a) electrostatic and hydrodynamic forces and (b) of relative pressure.

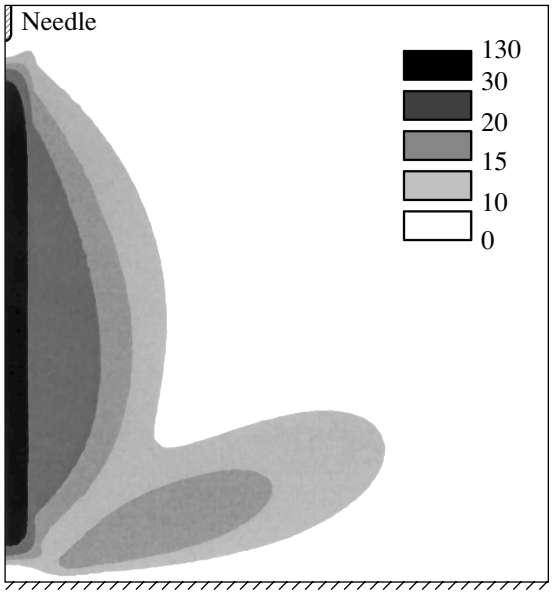

Fig. 7. Contour diagram of the values of the electric Reynolds number in the electrode gap.

a higher pressure (Fig. 6b). In the main part of the electrode gap, the differences in the forces and their absolute values are small and the flow is viscous and dissipative by nature (the driving force is balanced by the viscous drag). Immediately under the active electrode, a negative pressure region is located, in which the value of pressure (relative to the atmospheric pressure) is –360 Pa. In the remaining part of the electrode gap, the pressure is practically constant and increases considerably only in the immediate vicinity of the counter electrode.

The simulation was carried out under the assumption that the volume charge density is distributed uniformly in the central filament of the flow. Such an assumption is justified if the average drift velocity of ions is much lower than the velocity of the fluid (i.e., if the charge is frozen in the fluid). The results of direct verification of this condition are presented in Fig. 7, which shows the contour diagram of the electric Reynolds number in the electrode gap. The value of the Reynolds number was obtained as the ratio of the magnitude of the velocity of the fluid (in each element of the net) to the product of the values of electric field (in the same elements) and the mobility of ions. The region where the fluid velocity is more than ten times the drift velocity of ions is shown by dark color in the diagram. The width of this region is several times larger than the transverse size of the charged filament; consequently, the assumption concerning the uniformity of the charge density distribution in the filament can be regarded as justified.

EXPERIMENT AND ITS COMPARISON WITH THE COMPUTER MODEL

The natural experiment was carried out under the conditions coinciding with the computer model. Visualization of EHD flows and processing of experimental data were carried out in accordance with the technique described in [7].

Figure 8 shows contour diagrams of velocity obtained experimentally and as a result of simulation; the values of velocity are given in cm/s. Experimental data were processed using the original software (EHD reader) developed for processing EHD flows [8]. The graphs are qualitatively identical. The force region of the flow is localized in a narrow filament along the symmetry axis of the model. A significant decrease in the velocity is observed immediately at the surface of the counter electrode.

At the same time, detailed analysis of the graphs reveals some differences. For example, the lines of the maximal velocity level (30 cm/s) in the computer model are more extended in the direction of the normal to the plane electrode, while level lines 15 and 10 have a characteristic narrowing in the lower part. This features are due to the fact the computer model disregards migration spread of a charged filament moving across the electrode gap.

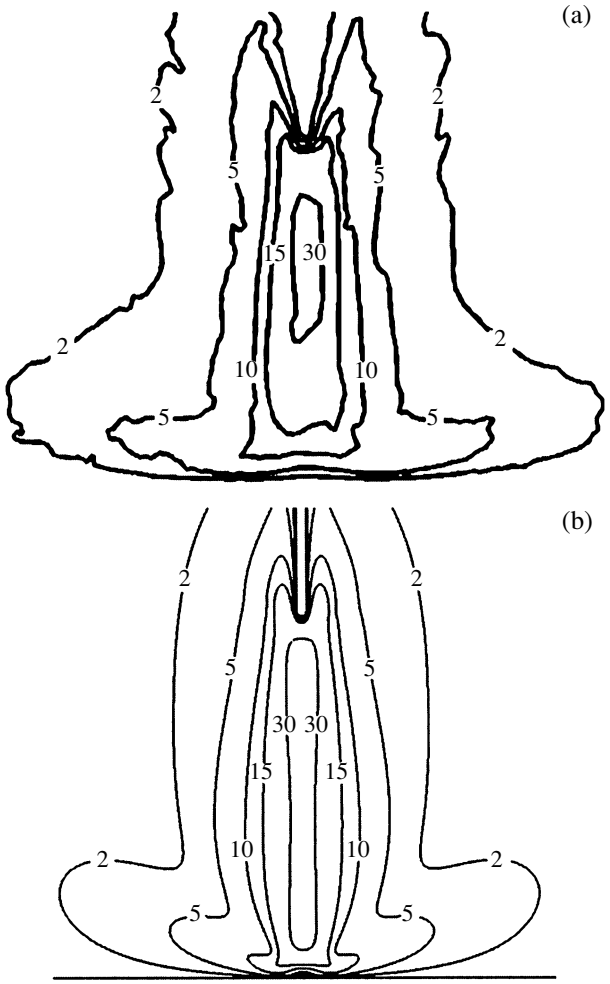

Fig. 8. Contour diagrams of velocity (a) experimental and (b) obtained as a result of simulation; values of velocity are given in cm/s.

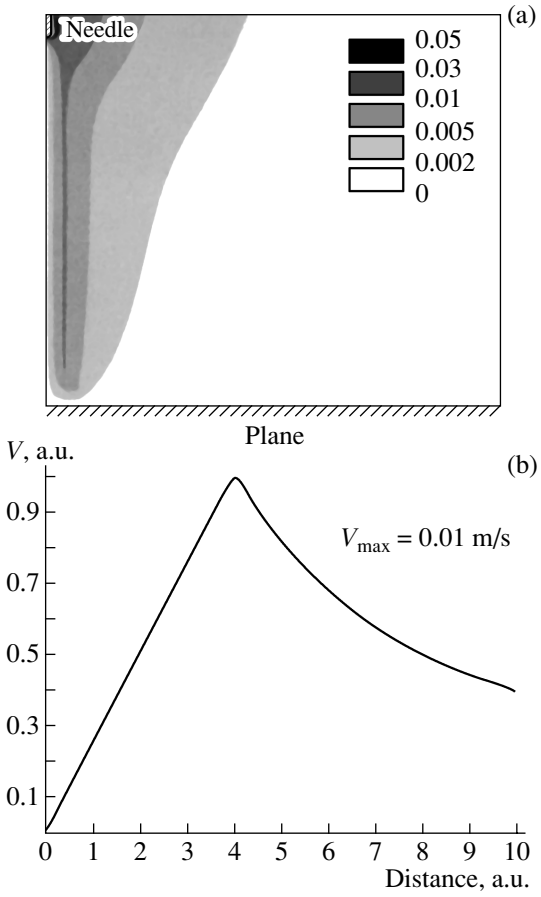

Fig. 9. (a) Contour diagram and (b) the graph of the x component of the drift velocity of ion (the latter is determined along the transverse path at the middle of the electrode gap).

In contrast to the wire–plane electrode system (for which the experimental results are in god agreement with experiment), a typical feature of EHD flows in the needle–plane electrode system is that the volume charge density has large values, which leads to the emergence of a strong transverse electric field. As a result, the drift velocity of ions directed across the fluid flow increases. For this reason, migration-induced spreading of the charged filament in its own transverse field apparently becomes noticeable in the lower part of the filament, which in turn is manifested in a decrease in the volume charge density and, hence, leads to a decrease in the forces acting on the fluid. As a result, a region of a smoother deceleration as compared to the model is observed in the experiment.

To confirm the assumption concerning the migration-induced spreading of the filament, we can put forth the following arguments. Figure 9 shows the graphs of the x component of the drift velocity (contour diagram and the curve plotted along the transverse path), calculated as the product of the mobility of ions in transformer oil and the electric field.

The characteristic time during which the fluid flowing with an average velocity of 30 cm/s traverses the electrode gap amounts to 0.02 s. Consequently, an ion must traverse during this time a distance of $\approx 0.0002m = 2r$ (i.e., a distance equal to two radii of the electrode, while the thickness of the charged region amounts to approximately four radii of the needle tip) exclusively due to the drift component of the velocity. An increase in the thickness of the region with a volume charge even by one radius of the needle will lead to an increase in the cross-sectional area of this region by a factor of 1.5 and, hence, to an analogous decrease in the volume charge density. Thus, in spite of the fact that the velocity of the fluid considerably exceeds the drift velocity of ions (by more than 30 times in the central filament), disregarding the latter velocity may noticeably affect the results.

CONCLUSIONS

In this paper, we comprehensively studied the structure of EHD flows in the needle–plane electrode system

on the basis of analysis of experimental data and the results of computer simulation. An iterative algorithm of simulation of the volume charge distribution in a fluid was worked out. The flexibility of its realization makes it possible to optimize it easily and, when necessary, take into account additional factors affecting the thickness of the charged region.

Our calculations enabled us to reveal a number of features of EHD flows in the needle–plane electrode system. First, the fluid flow is localized within a narrow central filament with a characteristic size on the order of several radii of the active electrode; outside this filament, the velocity of the fluid flow is much smaller than the maximal velocity. Second, a characteristic feature of EHD flows in the electrode system under investigation (in contrast to the wire–plane electrode system) is the large value of the volume charge density (on the order of 10^{-1} C/m^3). This leads to the emergence of a quite strong transverse electric field, which in turn necessitates the inclusion of the transverse component of the drift velocity of ions in simulation. Third, the presence of a region with a low pressure immediately under the needle electrode is worth mentioning.

REFERENCES

1. Yu. K. Stishkov and I. A. Elagin, Zh. Tekh. Fiz. **75** (9), 15 (2005) [Tech. Phys. **50**, 1119 (2005)].
2. Yu. K. Stishkov, V. L. Dernovskii, and A. A. Statuya, in *Proceedings of the 8th International Scientific Conference on Modern Problems of Electrophysics and Electrohydrodynamics of Liquids, St. Petersburg, 2006*, p. 206.
3. Yu. K. Stishkov and P. V. Glushchenko, in *Proceedings of the 8th International Scientific Conference on Modern Problems of Electrophysics and Electrohydrodynamics of Liquids, St. Petersburg, 2006*, p. 185.
4. Yu. K. Stishkov and V. A. Chirkov, in *Proceedings of the 8th International Scientific Conference on Modern Problems of Electrophysics and Electrohydrodynamics of Liquids, St. Petersburg, 2006*, p. 175.
5. A. V. Steblyanko and Yu. K. Stishkov, Zh. Tekh. Fiz. **67** (10), 105 (1997) [Tech. Phys. **42**, 1206 (1997)]; in *Proceedings of the 8th International Scientific Conference on Modern Problems of Electrophysics and Electrohydrodynamics of Liquids, St. Petersburg, 2006*, p. 59.
6. A. S. Lazarev and Yu. K. Stishkov, in *Proceedings of the 8th International Scientific Conference on Modern Problems of Electrophysics and Electrohydrodynamics of Liquids, St. Petersburg, 2006*, p. 59.
7. Yu. K. Stishkov and M. A. Pavleino, Elektron. Obrab. Mater., No. 1, 14 (2000).
8. S. B. Afanas'ev, D. S. Lavrenyuk, P. O. Nikolaev, and Yu. K. Stishkov, Elektron. Obrab. Mater., No. 1, 24 (2007).

Translated by N. Wadhwa

SPELL OK